

Elastic and piezoelectric constants of silver-iodide: Study of a material at the covalent-ionic phase transition

T. A. Fjeldly and R. C. Hanson*

Max Planck Institut für Festkörperforschung, Stuttgart, Federal Republic of Germany

(Received 2 May 1974)

We have studied the elastic and piezoelectric properties of AgI in the wurtzite phase. Transformed elastic constants for the zinc-blende phase are obtained and are compared with those of other covalently bonded compounds near Phillip's critical ionicity ($f = 0.785$). This confirms the earlier reported trend in the approach to zero of the $(C_{11} - C_{12})/2$ elastic constant as the covalent to ionic phase transition is approached, indicating a lattice instability owing to a vanishing of the bending force constant. The room-temperature hydrostatic pressure dependence of the elastic constants exhibits a peculiar hysteretic behavior, possibly related to a sluggish conversion from wurtzite to zinc-blende structure. The temperature dependence of the elastic constants is also reported. The piezoelectric constants were determined.

I. INTRODUCTION

Recently, there has been considerable interest in zinc-blende and wurtzite (wz) structure compounds with ionicity close to the critical value (0.785) described in Phillip's theory.¹ This critical ionicity serves as a well-defined crossover point between the compounds with tetrahedral covalent structures, and those with six or eight coordinated ionic bonding. Martin² brought attention to the fact that the elastic properties of the covalently bonded materials show a systematic tendency towards a lattice instability as the ionicity increases. This trend was more recently confirmed by Hanson *et al.*³ for the cuprous halides, which are some of the most ionic zinc-blende-structure compounds known (f_i between 0.692 and 0.746).

The tendency towards lattice instability in this class of materials is also indicated by the increase in anharmonicity. Hanson *et al.*⁴ have shown that CuCl ($f_i = 0.746$) has large negative pressure derivatives of the shear elastic constants. This explains the large negative thermal expansion at low temperatures. AgI exhibits a negative thermal expansion in the whole range from 0 to 300 K,⁵ so we expect that it will have similar anharmonic properties.

AgI as well as the cuprous halides all show phase transitions to more ionic structures at relatively low hydrostatic pressure. This again reflects the fact that these materials are all very near the covalent-ionic phase transition.⁶ In AgI, the transition from the wurtzite phase, which is stable at room temperature and pressure⁷ to the rock-salt phase, occurs at roughly 3 kbar, although there is a small region of another phase which occurs in the vicinity of 3 kbar.^{8,9}

In this work, we have directed our attention to the elastic and piezoelectric properties of the wurtzite modification of AgI. We have measured

absolute values, temperature dependence, and pressure dependence of the elastic constants. The absolute values are compared with those of the cuprous halides; and in particular, the effective cubic shear constant $\frac{1}{2}(C_{11} - C_{12})$ for this series of materials seems to extrapolate to zero at the critical ionicity. Of interest also is an anomalous hysteretic behavior found in the pressure dependence of the elastic constants. The phenomenon is possibly associated with the fact that AgI is dimorphous, and that there is some restacking of layers in the lattice taking place in the direction of conversion to zinc-blende structure. We are reporting elsewhere a related behavior in the shifts and intensities of the Raman spectra of wurtzite AgI under pressure, as well as Raman spectra of the other phases of AgI.¹⁰

II. EXPERIMENTAL

Single crystals of wurtzite structure AgI were grown from solution by a method similar to the one described by Latakos and Lieser.¹¹ Approximately 100-ml saturated solution of AgI in 67 wt% HI was carefully covered with an equal amount of methanol in a 300-ml beaker. A thin layer of concentrated HI between the methanol and the solution served to reduce precipitation at the interface when pouring in the methanol. The beaker was subsequently placed in a desiccator with a saturated methanol atmosphere, and left for the liquids to mix by diffusion for four weeks in a temperature-stabilized environment.

The crystals thus obtained were clear with a light yellow color, and were in the shape of pyramids pointing along the hexagonal axis. The biggest crystals had linear dimensions of typically 7–10 mm, but the average size was 3–4 mm.

AgI is very soft and flows easily. However, the

crystal cleaves readily in the hexagonal basal plane. Thus, the preparation of ultrasonic samples for propagation along the hexagonal axis was relatively easy. A sample was also prepared for sound propagation in the basal plane. The samples were in the form of plates ranging in thickness between 2.3 and 3.2 mm.

The various sound velocities and their temperature and pressure dependences were measured with a standard pulse-echo overlap technique.^{12,13} The experimental setup was built around a Matec 6000 rf pulse generator. The rf frequencies used were 20 and 30 MHz. The quartz transducers were bonded to the samples with Nonaq stop-cock grease or solid phenylsalicylate, "salol". The salol proved to give reliable bonds that normally did not break in the pressure experiments. Moreover, in checks with grease bonds, no errors in the data induced by the solid bonds were observed.

The hydrostatic pressure was achieved in a standard steel cell with an electrical feedthrough. Silicon oil was used as the pressure-transmitting liquid. It was pumped with a conventional two-stage pump that could deliver a pressure of maximum 7 kbar. The pressure was monitored with a calibrated manganin resistance cell. The temperature dependence of the sound velocities were measured in the range 15–300 K, and in one case up close to the phase transition at 147 °C.

To supplement the set of elastic stiffness constants derived from the ultrasound measurements, additional data on elastic compliances and stiffnesses were obtained at room temperature from mechanical resonance experiments in oriented bars and plates of AgI. By investigating the resonance and antiresonance frequencies of these vibrations, two of the electromechanical coupling constants could also be determined.¹⁴ In particular, from the length expander resonances in a long bar oriented along the z axis, the compliance S_{33} was determined. Similarly, from the lowest length expander resonance in a long bar oriented in the hexagonal basal plane, the compliance constant S_{11} was obtained. In this case, the electric field was applied in the z direction, perpendicular to the long axis. From a careful measurement of the frequencies of the resonance and associated antiresonance, the piezoelectric coupling constant k_{31} was determined. A second piezoelectric coupling constant, k_t , was obtained from the resonance-antiresonance structure of the longitudinal thickness modes in a plate oriented perpendicular to the z axis. The location of this resonance provided an independent determination of the elastic stiffness constant C_{33}^E . The coupling constant k_{15} was estimated from the difference between C_{44}^D and C_{44}^E measured by the pulse-echo method in the x and z directions, respectively. Finally, the hydrostatic pressure con-

stant d_h was measured using fast release of 1-kbar oil pressure and measuring the resultant charge across z faces.

III. RESULTS

A. Elastic constants

The measured and derived values for the hexagonal elastic stiffness and compliance constants are shown in Table I. The superscripts D (constant displacement) and E (constant electric field) refer to the piezoelectrically stiffened and unstiffened constants, respectively. When the superscript is omitted, the corresponding constant is unstiffened for all cases.

The most reliable data are the ultrasonic measurements of C_{33}^D , C_{44}^E , C_{11} , and C_{66} , and the compliances S_{33} and S_{11} obtained from the length expander modes. Using the electromechanical coupling constant k_t (Table III), we calculate the unstiffened constant C_{33}^E . From this set of unstiffened constants, all the remaining stiffnesses and compliances can be computed with one redundancy providing a check on the others. As S_{11} is the least certain of the set, this measurement was chosen as the check; and we find that its computed value 0.80×10^{-11} cm²/dyn agrees with the experimental one $[(0.79 \pm 0.03) \times 10^{11}$ cm²/dyn] to well within the experimental error limits.

The value for $C_{33}^D = 3.8 \times 10^{11}$ dyn/cm², obtained through the longitudinal thickness mode along z , is somewhat unreliable. Only one heavily damped resonance could be seen, resulting in a somewhat large uncertainty ($\pm 5\%$) in this number.

The large uncertainty in C_{44}^D occurs because the two shear waves propagating in the basal plane, giving C_{66} and C_{44}^D , are observed to have nearly the same velocities. The wave with polarization in the basal plane giving C_{66} was very much less attenuated than the wave giving C_{44}^D . Therefore, it was not possible to be sure that the observed echoes for C_{44}^D did not, in fact, have a slight admixture of C_{66} , which would, of course, affect considerably the

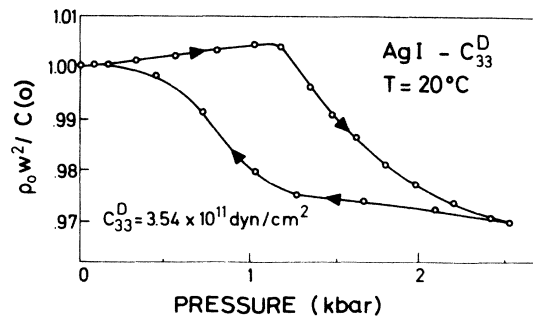


FIG. 1. Pressure dependence of the C_{33}^D elastic constant of AgI (wz).

TABLE I. Elastic stiffness and compliance constants of AgI (wurtzite) at 25°C and 10°K.

Constant	Propagation	Polarization	Elastic stiffness (10^{11} dyn/cm 2 = 10^{10} N/m 2)	
			$T = 25^\circ\text{C}$	$T = 10^\circ\text{K}$
C_{11}^a	x	x	2.93 ± 0.06	3.74 ± 0.07
C_{33}^D	z	z	3.60 ± 0.07	4.39 ± 0.08
C_{33}^E			3.54 ± 0.10	
C_{44}^E	z	x	0.373 ± 0.008	0.410 ± 0.010
C_{44}^D	x	z	0.40 ± 0.02	
C_{66}^a	x	y	0.399 ± 0.008	0.431 ± 0.010
C_{12}			2.13 ± 0.07	
C_{13}			1.96 ± 0.04	
			Elastic compliance (10^{-11} cm 2 /dyn = 10^{-10} m 2 /N) $T = 25^\circ\text{C}$	
S_{11}^a	length expan- der	x	0.79 ± 0.03	
S_{33}^a	length expan- der	z	0.49 ± 0.01	
S_{44}			2.68 ± 0.05	
S_{12}			-0.46 ± 0.01	
S_{13}			-0.19 ± 0.1	

^aMeasured quantity—others are computed.

tuning procedure used to obtain the absolute elastic constants.

As a final check, the various elastic constants measured or derived here can be used to compute the linear compressibilities. Using the values in Table I, the linear compressibilities for the z direction and for directions in the basal plane, are, respectively,

$$\beta_c = S_{33} + 2S_{13} = (1.1 \pm 0.1) \times 10^{-12} \text{ cm}^2/\text{dyn},$$

$$\beta_a = S_{11} + S_{12} + S_{13} = (1.5 \pm 0.2) \times 10^{-12} \text{ cm}^2/\text{dyn}.$$

The corresponding values found by Davis and Blair¹⁵ are $\beta_c = (1.09 \pm 0.32) \times 10^{-10} \text{ cm}^2/\text{dyn}$ and $\beta_a = (1.46 \pm 0.42) \times 10^{-10} \text{ cm}^2/\text{dyn}$. The agreement is again very good, a fact that also tends to confirm the choice of sign made earlier for C_{13} and S_{13} .

In Figs. 1–4, the rather curious hysteretic behavior in the pressure dependence of the elastic constants is shown. For clarity, solid lines have been drawn through the experimental points, and the arrows indicate the sequence of the measurements. The C_{33} curve in Fig. 1 is the first run on a freshly prepared crystal. The others were measured after at least one pressure cycle to about 2 kbar. The shape of the hystereses changed somewhat after each cycle, but qualitatively, the be-

havior remained the same. The slope of the linear portions was the same for each cycle. At each pressure point the sound velocity was only measured after temperature equilibrium was reached. For some points in the curve the velocity change was measured again after longer lapses of time ($\frac{1}{2}$ to 1 h) to see if further relaxation due to other mechanisms was present, but no further changes were

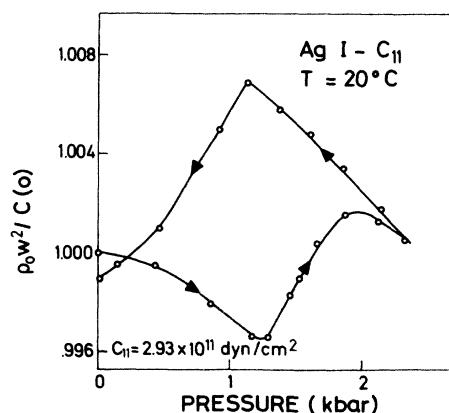


FIG. 2. Pressure dependence of the C_{11} elastic constant of AgI (wz).

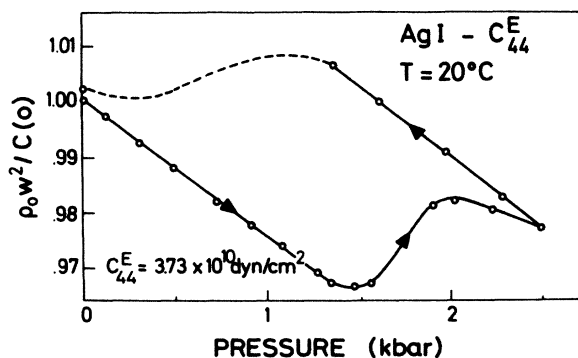


FIG. 3. Pressure dependence of the C_{44}^E elastic constant of AgI (wz).

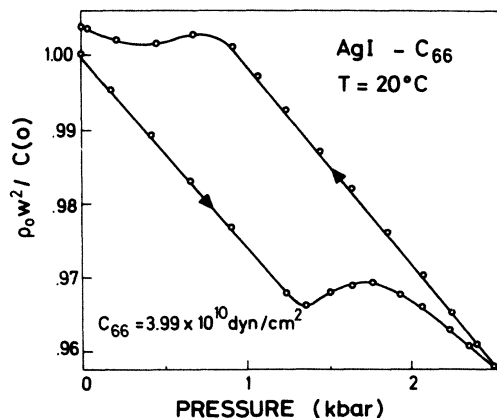


FIG. 4. Pressure dependence of the C_{66} elastic constant of AgI (wz).

seen.

The main loop of the hysteresis always describes approximately a parallelogram with the low-pressure corner between 0 and 0.4 kbar and the high-pressure corner at about 2 kbar. Above and partially also below this region, the experimental points for increasing and decreasing pressure have a tendency to come together. In one run on C_{33} , the sample was pressurized through the 3-kbar phase transition. The elastic constants changed smoothly all the way up to the phase transition, whereupon the crystal transformed abruptly and the ultrasonic signal disappeared. It is noteworthy that for three of the elastic constants, C_{11} , C_{66} , and C_{44}^E , the pressure coefficient is initially negative and the hysteresis loop is traversed in an anticlockwise sense. For C_{33}^D , the initial pressure coefficient is very close to zero and the loop has the opposite sense. The initial pressure coefficients for these elastic constants are listed in Table II. The raw data have here been corrected for the length changes caused by the hydrostatic pressure.

Finally, it should be mentioned, as a point of interest for the subsequent discussion of the pressure data, that in the range of ultrasonic frequencies used (20–30 MHz), no drastic change in the ultrasonic attenuation was evident. A systematic investigation of this point is now being undertaken.

In Figs. 5 and 6 are shown the temperature dependences of the four elastic constants C_{33}^D , C_{44}^E , C_{11} ,

and C_{66} . There is nothing remarkable about the behavior for any of these. The elastic constants all stiffen continuously on cooling to liquid helium from room temperature. The total change in this temperature range is about 20% for the two longitudinal constants, C_{11} and C_{33} , and somewhat less than 10% for the transverse constants, C_{44} and C_{66} . C_{11} was measured up to within 8° of the phase transition to the disordered phase without showing any signs of anomalous behavior. The temperature coefficients for the elastic stiffnesses at room temperature are listed in Table II.

B. Piezoelectric constants

The thickness longitudinal resonance in the z direction gave $k_t = (0.133 \pm 10\%)$. This mode was rather highly damped, although no evidence was seen for spurious resonances often seen in thickness modes. From this, the calculated $e_{33} = 0.20$ C/m² using a dielectric constant of 7.¹⁶ The length expander mode gives $k_{31} = 0.130 \pm 2\%$ from which one calculates $d_{31} = -9.1 \times 10^{-12}$ C/N. The sign of these various piezoelectric constants was not directly measured because the extreme softness of the crystals did not permit application of uniaxial stress. We assume that the sign of the piezoelectric constants are the same as for CdS (Ref. 17) since AgI is even more ionic than CdS and the re-

TABLE II. Logarithmic pressure and temperature derivatives of the elastic stiffness constants of wurtzite-structure AgI at 1 bar and 25°C. The value for C_{12} is computed from C_{11} and C_{66} .

	C_{11}	C_{33}	C_{12}	C_{44}	C_{66}
$\frac{1}{C} \frac{dC}{dp}$ (10^{-2} kbar ⁻¹)	-0.4 ± 0.4	0.0 ± 0.1	0.47	-2.7 ± 0.1	-2.7 ± 0.1
$\frac{1}{C} \frac{dC}{dT}$ (10^{-4} K ⁻¹)	-11.6 ± 0.3	-12.6 ± 0.4	-14.2	-6.1 ± 0.2	-4.6 ± 0.2

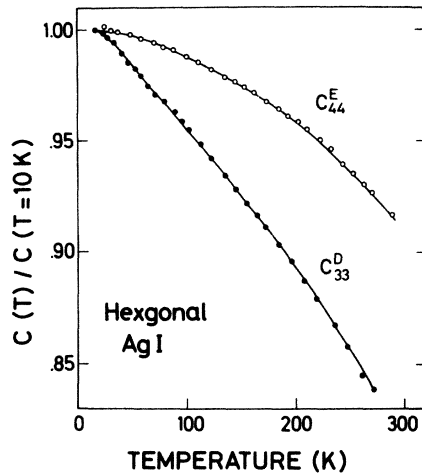


FIG. 5. Temperature dependence of the C_{44}^E and C_{33}^D elastic constants of AgI (wz).

versal of the sign in piezoelectric constants has only before been observed in the very covalent III-V compounds.¹⁸ The hydrostatic piezoelectric constant $d_h = d_{33} + 2d_{31}$ was also measured giving $d_h = +1 \times 10^{-12}$ C/N $\pm 30\%$. In this case, the sign was fixed using the crystallographic polarity determination of Bhalla *et al.*¹⁹ From these and the elastic constants, we calculate d_{33} and e_{31} .

We tried resonance measurements on plates perpendicular to x but we were unable to see the expected thickness shear resonances arising from coupling with the d_{15} piezoelectric constant. From the measurements of C_{44}^D and C_{44}^E , we obtain a rough estimate for $k_{15}' = (0.27 \pm 35)\%$ and $e_{15} = 0.13$ C/m² $\pm 35\%$. The large uncertainty here is due to the difficulties we had in measuring C_{44}^D . A summary of the piezoelectric results is given in Table III.

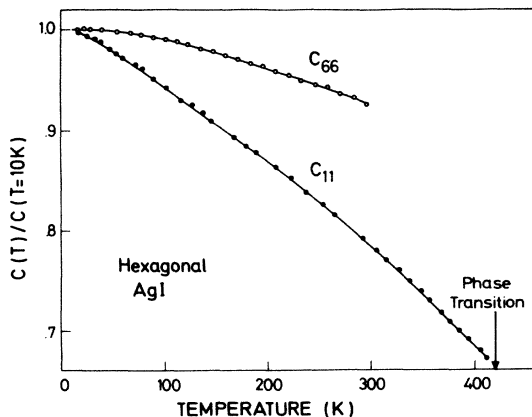


FIG. 6. Temperature dependence of the C_{66} and C_{11} elastic constants of AgI (wz).

TABLE III. Electromechanical coupling constants and piezoelectric constants of AgI; $T = 25^\circ\text{C}$.

k_t^a	0.133 ± 0.013
k_{31}^a	0.130 ± 0.005
$k_{15}'^a$	0.27 ± 0.10
e_{33}	$+0.20$ C/m ²
e_{31}	-0.078 C/m ²
e_{15}^a	$-(0.13 \pm 0.05)$ C/m ²
d_{33}	19.1×10^{-12} C/N
d_{31}^a	$-(9.1 \pm 0.6) \times 10^{-12}$ C/N
$d_h^{a,b}$	$+(1.0 \pm 0.3) \times 10^{-12}$ C/N

^aMeasured quantity.

^bSign for d_h was directly measured, others inferred.

IV. DISCUSSION

A. Elastic constants-magnitude

One objective for studying the elastic constants of AgI is to further investigate the trend towards elastic instability as the Phillip's critical ionicity is approached. This trend has already been established in zinc-blende materials² and especially in the cuprous halides.³ To do this comparison, it is necessary to perform a transformation of elastic constants from the wurtzite to the zinc-blende structure. Sullivan²⁰ and Martin²¹ have presented two approaches to this transformation. Their approaches are in some ways equivalent.

In Martin's theory²¹ the differences between the two structures for third and more distant neighbors are ignored, and the second neighbors are brought into eclipsing arrangement by simple rotation of the fundamental tetrahedral building blocks. This corresponds to rotations of the elastic tensor with an added internal strain parameter to account for the two inequivalently oriented sets of tetrahedra in wurtzite. Martin's transformation then permits the calculation of effective cubic elastic constants for the wurtzite material. He uses a least-squares fit to six wurtzite elastic constants in his transformation, although only five are independent. This, we feel, unduly emphasizes the constants C_{11} and C_{66} (or C_{11} and C_{12}), and we have therefore chosen to apply a transformation equivalent to Martin's, but with a least-squares fit to five independent hexagonal constants, C_{11} , C_{13} , C_{33} , C_{44} , and C_{66} . The resulting transformed cubic elastic constants for AgI are listed in Table IV.

Sullivan gives relations between the elastic constants of the two structures which are equivalent to Martin's except that the internal strain parameter is not included and the transformation as given is not a least-squares fit. The values obtained by

TABLE IV. Elastic constants of zinc-blende-structure AgI obtained by transformation of wurtzite constants; $T = 25^\circ\text{C}$.

Constant	Elastic stiffness (10^{11} dyn/cm $^2 = 10^{10}$ N/m 2)	
	Martin ^{a,d}	Sullivan ^{b,d}
C_{11}	2.62	2.47
C_{12}	2.29	2.27
C_{44}	0.817	0.91
$\frac{1}{2}(C_{11} - C_{12})$	0.161	0.10
B	2.405	2.34
β/α ^c no units	0.024	0.012

^aCalculated according to modified method of R. Martin (Ref. 21); see text.

^bCalculated according to method of Sullivan (Ref. 20).

^cRatio of bending to stretching force constants in model of R. Martin (Ref. 2) using the above elastic constants.

^dWhen these zinc-blende constants are retransformed back to wurtzite the deviations between the original and retransformed constants are (for the Martin and Sullivan transformations, respectively) $C_{11} + 3\%$, $+12\%$; $C_{33} - 1.5\%$, 0% ; $C_{13} - 5\%$, -12% ; $C_{44} - 17\%$, -1% ; $C_{66} - 11\%$, $+60\%$.

this method are also given in Table IV. In a footnote, we give the deviations from the actual wurtzite constants when the calculated zinc-blende constants are retransformed back to wurtzite. Note that the Martin transformation gives a considerably better fit for C_{66} which is a direct result of the inclusion of the internal strain in his treatment.

These elastic constants are divided by $C_0 = e^2/a^4 = 3.7 \times 10^{11}$ dyn/cm 2 to form the reduced elastic moduli.² e is the electronic charge and a is the nearest-neighbor distance. In Fig. 7 we show the reduced elastic constants for all zinc-blende structure materials and the transformed constants of AgI. In Fig. 8 we have plotted the reduced C_s for the cuprous halides and silver iodide versus ionicity. The error limits on the AgI values are the Martin and Sullivan values. We note that C_s is tending towards zero at the critical ionicity of 0.785. To realize the significance of this apparent instability in C_s , we take the model for the elastic constants of the zinc-blende structure which was derived by Martin.² In this model, $C_s = (3/2r)\beta + 0.0265SC_0$, where β is the "bending" force constant appropriate to $\Delta(\vec{r}_i \cdot \vec{r}_j)$ where \vec{r}_i and \vec{r}_j are bond vectors associated with different bonds around the same ion and $0.0265SC_0$ is the Coulomb contribution. In the case of AgI, $0.0265SC_0 = 0.036 \times 10^{11}$ dyn/cm 2 , so it would appear that C_s being in the range of 0.10×10^{11} to 0.16×10^{11} dyn/cm 2 , is approaching the absolute lower limit set by the Coulomb forces. All the other elastic constants involve α which is the "stretching" force constant

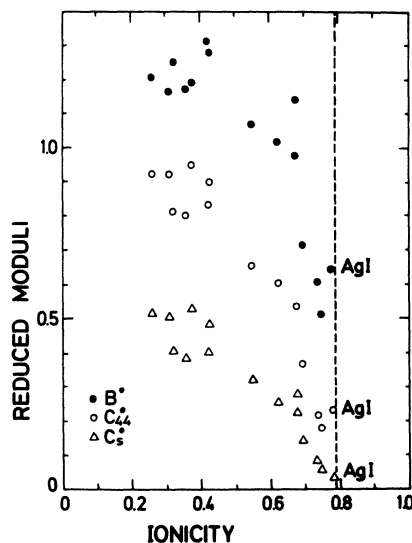


FIG. 7. Reduced elastic constants of zinc-blende structure materials and transformed AgI constants vs Phillips's ionicity. New values are for AgI immediately to left of dashed line which is the critical ionicity (0.785). Other values from Refs. 2 and 3.

associated with just the change in bond lengths. These other elastic constants become softer in these materials but not as much as C_s . The Coulomb part may tend to set a lower limit to C_s and prevent it from actually approaching zero at the critical ionicity. This would be consistent with the fact that the phase transition between the covalent and ionic structures is of first order. In the wurtzite structure, neither of the shear constants, C_{44} , nor $C_{66} = \frac{1}{2}(C_{11} - C_{12})$, depend simply on a bond-bending force constant so these constants do not reflect so dramatically the decrease in the bending force constant β . For AgI in this model² the ratio of the bending to stretching force constant,

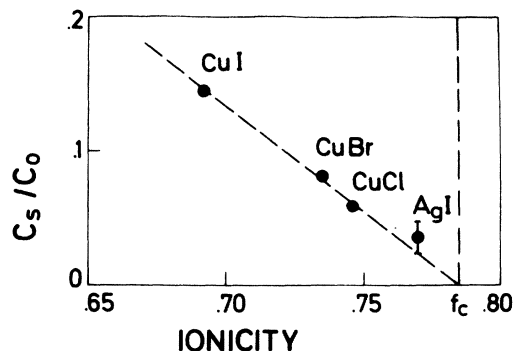


FIG. 8. Reduced $C_s = \frac{1}{2}(C_{11} - C_{12})$ elastic constant for cuprous halides (Ref. 2) and zinc-blende silver iodide versus Phillips's ionicity showing linear decrease to zero in this constant as critical ionicity is approached.

β/α , in the range 0.024–0.012. This represents the lowest value that this ratio achieves in any tetrahedrally bonded crystal.

We calculate the Debye temperatures from the low-temperature wurtzite elastic constants using the Legendre polynomial method of Betts *et al.*²² We estimate C_{13} at low temperature to be 2.38×10^{11} dyn/cm² using the temperature derivative of the relation given by Sullivan, $(d/dT)(C_{11} + C_{12} - C_{33} - C_{13}) = 0$, and assuming that the total change in elastic constants is proportional to the temperature derivative. The value of the Θ_D we obtain is 114 K. This compares with values of 119 and 116 K obtained by Burley²³ from x-ray and specific-heat data.

B. Elastic constants–temperature and pressure dependence

The temperature dependence of the elastic constants shows a normal stiffening with decreasing temperatures. The magnitudes of the temperature derivatives are comparable to those of CuCl.⁴

The pressure derivatives determined in the 1-bar to 1-kbar region are free of hysteresis effects. The shear constants show the expected negative pressure derivatives. The pressure derivative of the longitudinal constants is strange in that C_{11} has a slight negative pressure derivative and C_{33} has a zero derivative. If we ignore the anisotropy in the linear compressibility and compute mode gammas for these modes in the same way as for a cubic crystal, we obtain $\gamma = -3$ for both C_{44} and C_{66} . We can directly compare this with the mode gamma for shear waves propagating along the trigonal axis, $\langle 111 \rangle$, in zinc-blende-structure crystal. For CuCl (Ref. 4) this is -1.4 which is the most negative γ of zinc-blende-structure crystals. In our Raman work on AgI,¹⁰ we see a similarly defined mode gamma of -7.5 for the zone edge TA mode and for the related E_2 mode. Presumably, these negative mode gammas would explain the negative thermal expansion observed in AgI, especially in the low-temperature region.

We attempted to perform a transformation of these pressure derivatives to effective zinc-blende derivatives. We made an estimate of the pressure derivative of C_{13} using a procedure similar to the one we used above for the temperature derivative. However, when performing this transformation according to the Martin²¹ or Sullivan²⁰ methods we get an extremely large range of values with the sign not being uniquely determined except for C_s . The mode gamma for C_s comes out very large and negative in the range of -10 to -20 ! This compares with the mode gamma for C_s for CuCl (Ref. 4) which is -1.9 . It would be extremely interesting to measure this pressure derivative on the zinc-blende form but because of the lack of crystals

larger than a few microns, this appears to be impossible.

C. Elastic constants–hysteresis with pressure

It is apparent that further investigation is necessary in order to explain satisfactorily the peculiar hysteresis displayed in the pressure dependence of the elastic constants. We shall therefore at this point limit ourselves to make a few speculative remarks on the subject.

We report elsewhere¹⁰ on a related pressure behavior of the 17-cm^{-1} E_2 Raman mode. This mode, which can be regarded as the back-folded zone-edge transverse acoustical phonon at the L point in the zinc-blende structure, decreases drastically in intensity above 1 kbar and comes back with a sluggish hysteresis as the pressure is released, very similar to the hysteresis we observe here. These behaviors, which undoubtedly are related, suggest that the crystal transforms on a microscopic scale to zinc-blende structure. In experiments where AgI is pressurized into any of the high-pressure phases, it is known to return in the zinc-blende modification.⁹ In the present case, although no phase boundaries are crossed, a similar but hysteretic effect seems to take place. This may mean that within the dimorphous phase region the wurtzite structure is energetically more favorable at low pressures, while the zinc-blende structure is favored above about 1 kbar. However, disturbing to this hypothesis is the fact that the ultrasonic attenuation does not show any substantial increase under pressurization. Since the wurtzite to zinc-blende transformation is expected to be a reconstructive one, a large increase in ultrasonic attenuation should be found. However, the silver atoms in AgI are known to be notoriously mobile, presenting the outside possibility that a sluggish displacive-type transformation may take place. Hoshino and Shimoji²⁴ and Hara, Mori, and Ishiguro²⁵ have reported an increase in the ionic conductivity of wurtzite-phase AgI in this pressure range. It would be interesting to see if this change in the ionic conductivity shows the same hysteresis. Further investigation of the phenomenon such as careful x-ray studies, measurements of indices of refraction, and further ultrasonic and Raman studies over a larger frequency and temperature range, should yield information to clarify the mechanisms behind the present observations.

D. Piezoelectric constants

We shall discuss the magnitudes in terms of the e , stress, piezoelectric constants. We first note that the relation $-\frac{1}{2}e_{33} = e_{31} = e_{15}$ ¹⁷ that generally holds in wurtzite structure crystals, partially breaks down in the present case. The reason for this is not evident although, of course, under hydrostatic

pressure the material compresses 40% more along the basal directions than it does in the z direction as we have shown earlier.

We shall discuss the magnitude in relation to other materials using e_{33} since this is simply related to e_{14} in zinc-blende structure crystals ($e_{14} = e_{33}/\sqrt{3}$). In Martin's²⁶ formulation (a^2/e) $e_{14} = \zeta(e_T/e) - \Delta Q$, where a is the cubic-cell constant, e is the electronic charge, ζ is the internal strain, e_T is the Born effective charge, and Q is the charge transfer term.

For AgI, $a^2 e_{33}/\sqrt{3} e = a^2 e_{14}/e = 0.302$. We assume, following the trend of the cuprous halides,³ that $\zeta = 0.9$. From Bottger and Geddes¹⁶ $e_T/e = 1.40$. This gives $\zeta e_T/e = 1.26$ so ΔQ must be of the order of 0.96. This is to be compared with $\Delta Q = 0.14$ for CuCl, 0.54 for CuBr, and 0.47 for CuI. It is apparent that the charge transfer term is not scaling towards zero as the critical ionicity is approached. Since AgI is more ionic than CuCl but has a much larger ΔQ , it appears that the piezoelectric constant is smaller for the iodides and larger for the chlorides.

V. CONCLUSION

We have measured the absolute values, the pressure dependence, and the temperature dependence of the elastic constants in the wurtzite phase of AgI. In the same phase we also determined the values of the piezoelectric constants.

The absolute elastic constants were converted to effective cubic constants and compared with those of zinc-blende-structure compounds with high ionicity, in particular the cuprous halides. This comparison confirmed the trend towards lattice instability as the critical Phillips ionicity ($f_i = 0.875$) is approached. Particularly, the cubic shear constant

$C_s = (C_{11} - C_{12})/2$, which largely measures the atomic bond-bending force constant, clearly displays this effect. The ratio of the bending to stretching force constant, β/α , is in the range 0.024–0.012. It appears that the piezoelectric constant in contrast to the C_s elastic constant is not scaling simply with the ionicity.

The pressure dependence of the elastic constants had an interesting hysteretic behavior. This was tentatively interpreted as being related to a sluggish conversion to zinc-blende structure and back to wurtzite during a pressure cycle. This point clearly needs further elucidation through other experiments. The pressure derivatives of the elastic constants were measured in the region of small pressures free of hysteresis effects. The shear constants had the expected negative pressure derivatives, but so did the longitudinal constant C_{11} , while C_{33} had a zero derivative.

The temperature dependence of the elastic constants showed a normal softening of the constants with increasing temperature.

Two of the piezoelectric constants, e_{33} and e_{31} , were determined with reasonable accuracy from mechanical resonances and antiresonances in oriented bars and plates of AgI. The third constant, e_{15} , was roughly estimated from ultrasonic measurements. The magnitudes of the constants are comparable to those of cuprous iodide, but not cuprous chloride.

ACKNOWLEDGMENTS

We would like to thank Professor N. A. Fletcher for furnishing some of the crystals used in this investigation. We acknowledge helpful discussions with Professor M. Cardona and Dr. Richard Martin.

*On sabbatical leave from: Physics Dept., Arizona State University, Tempe, Ariz.—partially supported by the National Science Foundation Grant No. GP 29719.

¹J. C. Phillips, *Rev. Mod. Phys.* **42**, 317 (1970).

²R. M. Martin, *Phys. Rev. B* **1**, 4005 (1970).

³R. C. Hanson, J. R. Hallberg, and C. Schwab, *Appl. Phys. Lett.* **21**, 490 (1970).

⁴R. C. Hanson, K. Helliwell, and C. Schwab, *Phys. Rev. B* **9**, 2649 (1974).

⁵A. Bienenstock and G. Burley, *J. Phys. Chem. Solids* **24**, 1271 (1963).

⁶J. C. Phillips, *Phys. Rev. Lett.* **27**, 1197 (1971).

⁷G. Burley, *J. Phys. Chem.* **68**, 1111 (1964).

⁸B. L. Davis and L. H. Adams, *Science* **146**, 519 (1964).

⁹W. A. Bassett and T. Takahashi, *Am. Mineral.* **50**, 1576 (1965).

¹⁰R. C. Hanson and T. A. Fjeldly (unpublished).

¹¹E. Lakatos and K. H. Lieser, *Z. Phys. Chem. Neue Folge* **48**, 5228 (1966).

¹²E. P. Papadakis, *J. Acoust. Soc. Am.* **42**, 1045 (1967).

¹³D. H. Chung, D. J. Silversmith, and B. B. Chick, *Rev. Sci. Instrum.* **40**, 718 (1969).

¹⁴D. Berlincourt, D. Corran, and H. Jaffe, in *Physical Acoustics*, edited by W. P. Mason (Academic, New York, 1964), Vol. IA, p. 170.

¹⁵B. L. Davis and D. N. Blair, *J. Geophys. Res.* **73**, 6019 (1968).

¹⁶G. L. Bottger and A. L. Geddes, *J. Chem. Phys.* **46**, 3000 (1967).

¹⁷D. Berlincourt, H. Jaffe, and I. Shiozawa, *Phys. Rev.* **129**, 1009 (1963).

¹⁸G. Arlt and P. Quadflieg, *Phys. Status Solidi* **25**, 323 (1968).

¹⁹A. S. Bhalla, S. K. Suri, and E. W. White, *J. Appl. Phys.* **42**, 1833 (1971).

²⁰J. J. Sullivan, *J. Phys. Chem. Solids*, **25**, 1039 (1964).

²¹R. M. Martin, *Phys. Rev. B* **6**, 4546 (1972). Note that there are two errors which have been corrected here.

Equation (15) should be $Q = (1/3\sqrt{2}) [1 - 1 - 2]$ and in
Eq. (17) $D_3 = \Delta^2 \bar{S}_{11}^{yz}$.

- ²²D. D. Betts, A. B. Bhatia, and G. K. Horton, Phys. Rev. 104, 43 (1956).
- ²³G. Burley, J. Phys. Chem. Solids, 25, 629 (1964).
- ²⁴H. Hoshino and M. Shimoji, J. Phys. Chem. Solids 33, 2303 (1972).
- ²⁵M. Hara, T. Mori, and M. Ishiguro, Jpn. J. Appl. Phys. 12, 343 (1973).
- ²⁶R. M. Martin, Phys. Rev. B 5, 1607 (1972).